"In presenting the dissertation as a partial fulfillment of the requirements for an advanced degree from the Georgia Institute of Technology, I agree that the Library of the Institution shall make it available for inspection and circulation in accordance with its regulations governing materials of this type. I agree that permission to copy from, or to publish from, this dissertation may be granted by the professor under whose direction it was written, or, in his absence, by the dean of the Graduate Division when such copying or publication is solely for scholarly purposes and does not involve potential financial gain. It is understood that any copying from, or publication of, this dissertation which involves potential financial gain will not be allowed without written permission.

RADIANT ENERGY EXCHANGE

CONFIGURATION FACTORS FOR NON-LAMBERTONIAN SURFACES

A THESIS

Presented to

the Faculty of the Graduate Division

by

Roy Warner Blanton, Jr.

In Partial Fulfillment

of the Requirements for the Degree

Master of Science in Mechanical Engineering

Georgia Institute of Technology

April, 1959

RADIANT ENERGY EXCHANGE

CONFIGURATION FACTORS FOR NON-LAMBERTONIAN SURFACES

Approved

Dr. K. G. Picha, Chairman

Dr. C. W. Gorton

Dr. J. N. Hunt

Date Approved by Chairman 5/19/59

ACKNOWLEDGEMENTS

At the completion of this work, the author would like to make the following acknowledgements: To Dr. K. G. Picha, my advisor, for suggesting the problem and aiding with its solution; to Dr. C.W. Gorton, for his patient assistance and aid with the preparation of this manuscript; to Dr. J. N. Hunt, for editing the manuscript; and to the staff of the Rich Electronic Computer Center for their invaluable assistance with the numerical calculations.

TABLE OF CONTENTS

Page

ACKNOWLEDGEMENTS ii

LIST OF TABLES iv

LIST OF ILLUSTRATIONS v

Chapter

I. INTRODUCTION TO THE PROBLEM 1

II. DEVELOPMENT OF A NON-LAMBERTONIAN CONFIGURATION FACTOR 3

III. SOLUTION OF THE EQUATION 8

IV. DISCUSSION OF RESULTS 13

V. CONCLUSIONS AND RECOMMENDATIONS 16

APPENDIX 17

I. CONFIGURATION FACTOR BETWEEN AN ELEMENTAL AREA AND A PARALLEL DISK 18

II. CONFIGURATION FACTOR BETWEEN PERPENDICULAR PLANES . 22

III. DATA 26

BIBLIOGRAPHY 29

LIST OF TABLES

Table Page

1. Tabulated Data, Disk and Elemental Area 26

2. Tabulated Data, Perpendicular Planes 26

LIST OF ILLUSTRATIONS

Figure		Page
1.	Geometry for Configuration Factor Between Two Plane Point Sources	4
2.	Comparison of Analytical Expression for $\epsilon(\theta)$ with Data from Schmidt and Eckert	10
3.	Geometry for Configuration Factor Between Elemental Area and Parallel Disk	18
4.	Geometry for Configuration Factor Between Perpendicular Planes	22
5.	Shape Factor for Disk and Elemental Area	27
6.	Shape Factor for Perpendicular Planes	28

CHAPTER I

INTRODUCTION TO THE PROBLEM

The configuration factor F_{12} is defined to be the fraction of the total heat flux leaving an area A_1 that is incident upon another area, A_2. Its calculation is essential to the solution of all problems in radiant energy transfer. The usual approximate approach to the radiant energy transfer problem is to assume a Lambertonian surface, and then calculate the configuration factor, as a function only of the geometry involved in the problem.

A Lambertonian surface is one which radiates energy with equal intensity in all directions. A non-Lambertonian surface, however, has a radiation intensity that varies with angular direction. This variation of emissivity with angular direction was obtained for several materials by Schmidt and Eckert (1). Hamilton and Morgan (2) have proposed the use of Eckert's method (3) for the calculation of the configuration factor if additional accuracy is desirable. Eckert's method considers the intensity to be a function of the angular direction. The intensity is then integrated over the surface in the same manner as the configuration factor for the Lambertonian surface.

For the non-Lambertonian surface, the configuration factor is not merely a function of the geometry of the problem as will be shown later. Therefore a correction for the variation of emissivity

with angular direction must be applied. The application of this correction will yield results which differ from those obtained previously by Hamilton and Morgan (2). In their study, they considered several geometries and evaluated the configuration factors; however, all of the data they present is based on an assumed Lambertonian surface.

It is the purpose of this investigation to utilize the variation of emissivity with angular direction, as given by Schmidt and Eckert (1), to obtain an expression for the configuration factor of a non-Lambertonian surface. This expression is utilized in calculating, by numerical methods, the configuration factor for two geometries. The numerical computations were carried out on the IBM 650. The results for the non-Lambertonian surfaces are compared with those for the Lambertonian surfaces, and an indication of the error involved in assuming a Lambertonian distribution is shown.

CHAPTER II

DEVELOPMENT OF A NON-LAMBERTONIAN CONFIGURATION FACTOR

The configuration factor F_{12} from an area A_1 to another area, A_2 is defined to be the fraction of the total heat flux leaving A_1 that is incident upon A_2. The configuration factor equation, for a radiating plane source dA_1, and an intercepting plane area dA_2, is developed from Fig. 1 and the definition of the configuration factor as follows:

$$dA_1\ dF_{dA_1\ dA_2} = \frac{dq_{dA_1 \rightarrow dA_2}}{dq_{dA_1}} = \frac{i(\theta_1)\ dA_1 \cos \theta_1\ d\omega_1}{i_m \pi}$$

where $i(\theta_1)$ is the intensity at the angle θ_1 measured from the normal to the plane point source where the solid angle $d\omega_1$ is defined by:

$$d\omega_1 = \frac{dA_1 \cos \theta_2}{r^2}$$

and where i_m is the mean value of the intensity defined by

$i_m = e/\pi$ where e is the engegy emitted.

Now, using the notation of Hamilton and Morgan (2) the directional distribution function D (θ) is defined as:

$$D_1\ (\theta_1) = i\ (\theta_1)/i_m$$

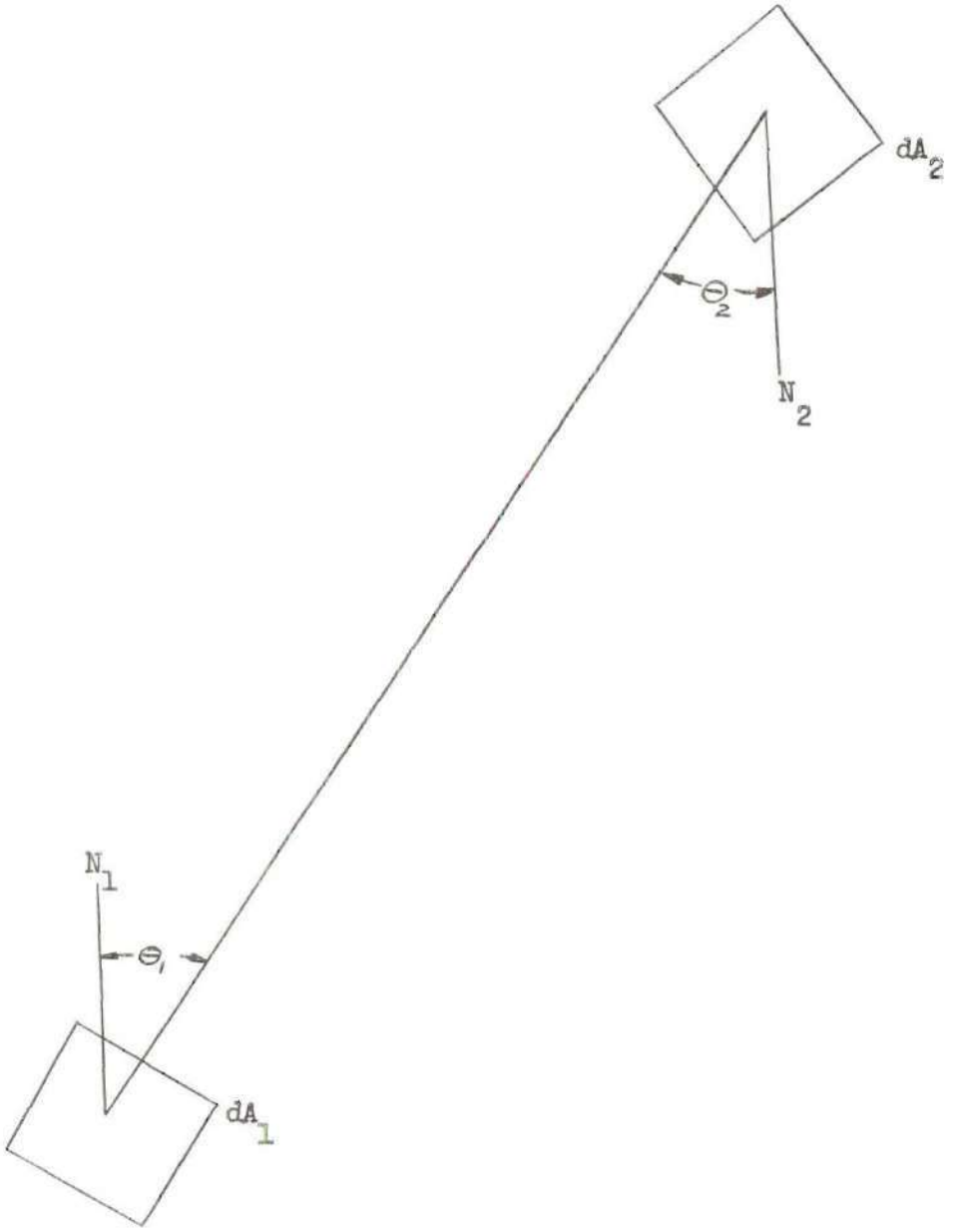

Figure 1. Geometry for Configuration Factor Between Two Plane Point Sources

Then it follows that

$$dA_1\, dF_{dA_1 dA_2} = \frac{D_1(\theta_1)\cos\theta_1 \cos\theta_2\, dA_1\, dA_2}{\pi r^2} \qquad (1)$$

The configuration factor F_{12} may now be found as soon as $D_1(\theta_1)$ is known by integrating over the surfaces A_1 and A_2. Now $\epsilon(\theta)$, the emissivity at the angle θ, must be defined in order to evaluate $D_1(\theta_1)$. Eckert (8) defines $\epsilon(\theta)$, the one directional emissivity by the relation

$$\epsilon(\theta) = \frac{i(\theta)}{i(b)}$$

where $i(b)$, the intensity of a black body, is a constant.[1] Then it follows that

$$i(\theta) = \epsilon(\theta)\, i(b)$$

Now for a black body, the emissive power, $e(b)$, can be found from the definition of intensity, i.e. $i = \frac{d e}{d \omega}$ and Lambert's Cosine Law, or

$$e(b)\int_0^{\pi/2} i(b)\cos\theta\, d\omega = 2\pi i(b)\int_0^{\pi/2} \sin\theta\cos\theta\, d\theta$$

$$e(b) = \pi\, i(b)$$

[1] The intensity of a black body is sometimes treated as a variable. As an example see Eckert (8).

then

$$i(b) = \frac{e(b)}{\pi}$$

and

$$i(\theta) = \frac{\epsilon(\theta)\, e(b)}{\pi}$$

and

$$i_m = \frac{e}{\pi} = \frac{\epsilon_1\, e(b)}{\pi}$$

by the definition of ϵ_1.

The hemispherical emissivity ϵ_1 is defined by

$$\epsilon_1 \quad \frac{e}{e(b)}$$

where

$$e = \int i \cos\theta \, d\omega = \int \epsilon(\theta)\, i(b) \cos\theta \, d\omega$$

$$e = 2\pi i(b) \int_0^{\pi/2} \epsilon(\theta) \sin\theta \cos\theta \, d\theta$$

so

$$\epsilon_1 = \frac{e}{e(b)} = \frac{2\pi\, i(b) \int_0^{\pi/2} \epsilon(\theta) \sin\theta \cos\theta \, d\theta}{\pi\, i(b)}$$

or

$$\epsilon_1 = 2 \int_0^{\pi/2} \epsilon(\theta) \sin\theta \cos\theta \, d\theta$$

Then it follows that

$$D_1(\theta_1) = \frac{\epsilon(\theta_1)\, e(b)/\pi}{\epsilon_1\, e(b)/\pi} \qquad \frac{\epsilon(\theta_1)}{\epsilon_1}$$

The non-Lambertonian configuration factor is given by

$$F_{12} = \frac{1}{\pi \epsilon_1 A_1} \int_{A_1}\int_{A_2} \frac{\epsilon(\theta_1)\cos\theta_1 \cos\theta_2 \, dA_1 \, dA_2}{r^2} \tag{2}$$

Likewise:

$$F_{21} \quad \frac{1}{\pi \epsilon_2 A_2} \int_{A_2}\int_{A_1} \frac{\epsilon(\theta_2)\cos\theta_1 \cos\theta_2 \, dA_1 \, dA_2}{r^2} \tag{3}$$

The angular emissivity for certain solids, may now be found, from Schmidt and Eckert (1), as a function of θ. With this substitution, F_{12} becomes once again, merely a function of the geometry of the problem.

Two things should be pointed out about equations (2) and (3). First, reciprocity need hold only as a special case, and second, for the case of the Lambertonian surface, these equations are identical with the classical configuration equation.

CHAPTER III

SOLUTION OF THE EQUATION

It was noted from Schmidt and Eckert (1) that the emissivity of electrical non-conductors follows very closely the Lambertonian distribution, whereas the emissivity of the electrical conductors deviates considerably from the Lambertonian distribution for values of θ greater than 45 degrees. For this reason a representative electrical conductor was selected, in preference to a non-conductor, from the five conductors presented by Schmidt and Eckert (1). Chromium was chosen and an equation was derived to fit the curves since no equation is given in the paper to correlate the data.

An approximate equation was fitted to the curve for chromium in two parts, $0 \leq \theta \leq 36.9$ degrees and 36.9 degrees $\leq \theta \leq 89.9$ degrees. The remainder of the solution may be neglected since cos θ in this range is near zero which makes equation (1) approximately zero. Examination of the data shows the first part of the equation to have a constant value, while the second part appears to be an exponential. When Log $\in(\theta)$ is plotted versus Log θ, the second part of the equation becomes a linear plot. A function, equation (5), was chosen which closely fitted this straight line.

Using the laws of logarithms to obtain the power of the exponent, the resulting approximate equations are:

$$\epsilon(\theta) = 0.0583 \qquad 0 \leq \theta \leq 0.6440 \tag{4}$$

and

$$\epsilon(\theta) = 0.0583 \left(\frac{0.3753}{\cos^2\theta \sin\theta} \right)^{1/3} \qquad 0.6440 \leq \theta \leq 1.5621 \tag{5}$$

where θ is given in radians. Fig. 2 shows how equations (4) and (5) fit the experimental values from Schmidt and Eckert (1).

Applying equations (2), (4), and (5) to the case of an elemental area and a parallel disk (radius a) separated by a distance b (see Appendix I), the following results are obtained:

$$F_{12} = \frac{1}{\pi \epsilon_1} \left[C_1 \int_0^{0.75b} \frac{b^2 2\pi \rho \, d\rho}{r^4} + C_2 \int_{0.75b}^{a} \frac{b^2 \, 2\pi \rho \, d\rho}{(b^2 \rho)^{1/3} r^3} \right] \tag{6}$$

if $0.75b < a$

and

$$F_{12} = \frac{C_1}{\epsilon_1} \frac{a^2}{a^2 + b^2} \qquad \text{if } 0.75\,b \geq a \tag{7}$$

where $C_1 = 0.0583$, $C_2 = 0.04205$, and $r \sqrt{b^2 + \rho^2}$.

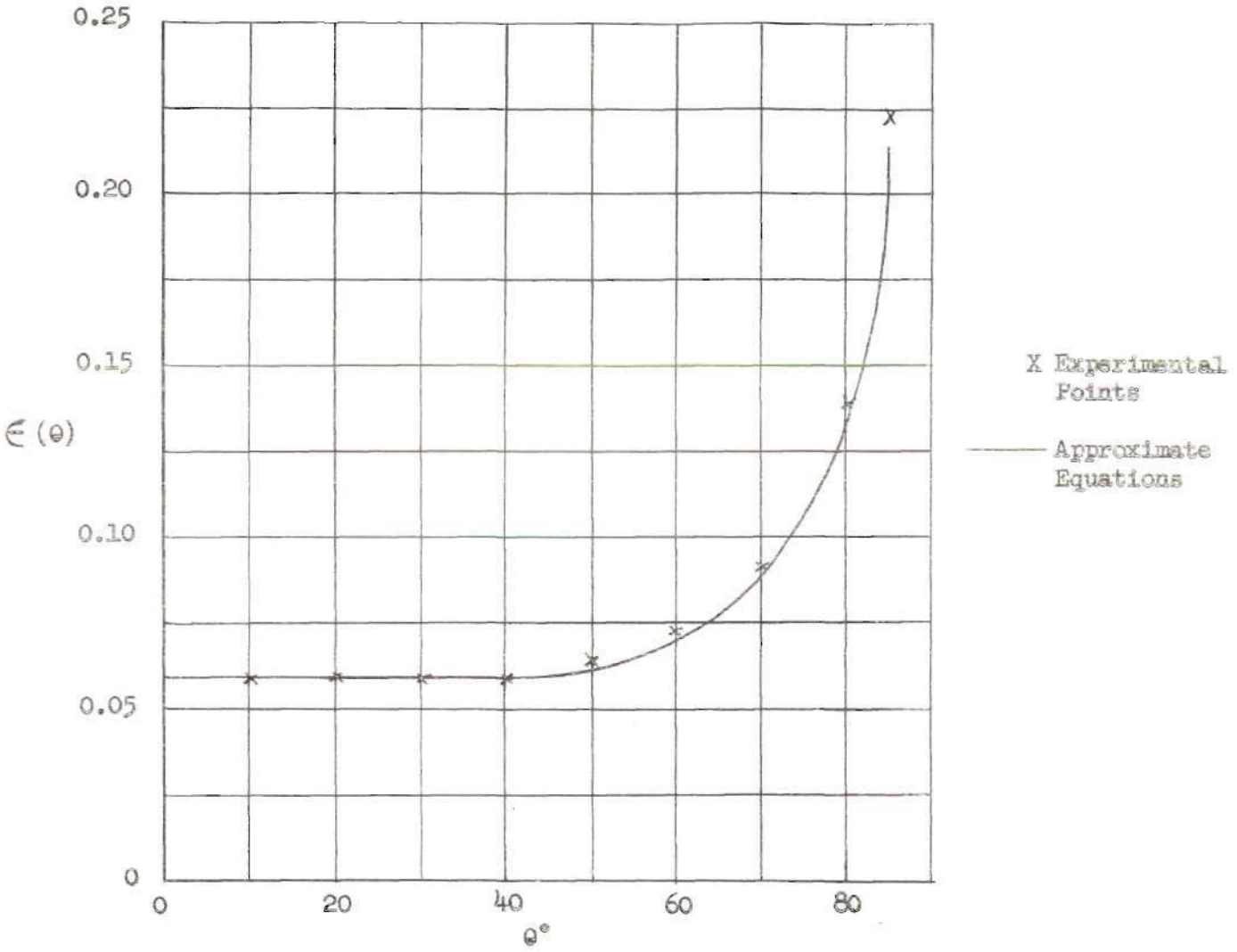

Figure 2. Comparison of Analytical Expression for $\epsilon(\theta)$ with Data From Schmidt and Eckert

The second integral of equation (6) may be reduced to the difference of two incomplete Beta functions; however, the limits of integration are outside the present range of tabulated values for the incomplete Beta function.

Equation (7) and the first part of equation (6) are readily evaluated by conventional methods; however, the last part of equation (6) required some special treatment. It was noted that the selection of b/a as a parameter would reduce the solution, when plotted, to a single curve. Then if a = 1, F need only be evaluated for several values of b. This was done with the aid of the IBM 650 Data Processing Machine and a program which was written in the Bell General Purpose System. With this program, the last part of equation (6) was evaluated by use of Simpson's Rule for the numerical integration with an increment, $\Delta \rho = 0.025$. The results of this work appear in Appendix III.

The second case considered was that of perpendicular planes with one edge in common (see Appendix II). When equations (2), (4), and (5) were applied to this case the following equations resulted:

$$X = \frac{C_1}{\pi \epsilon_1 \ell w} \int_{A_1} \int_{A_2} \frac{yz dx_1 \, dx_2 \, dydz}{r^4} \qquad (8)$$

if $0.79968 \leq y/r \leq 1$

and

$$Y \quad \frac{C_2}{\pi \epsilon_1 \ell w} \int_{A_1} \int_{A_2} \frac{y^{1/3} z dx_1 \, dx_2 \, dy \, dz}{\left[(x_1 - x_2)^2 + z^2 \right]^{1/6} r^3} \qquad (9)$$

if $0 < y/r \leq 0.79968$

where $F_{12} = X + Y$.

Equations (8) and (9) are similar in nature to equations (6) and (7) in that their solution may be simplified by the use of two parameters, $L = h/w$ and $M = \ell/w$. These will reduce the solution, when plotted, to a single family of curves. Only one of these curves, $M = 1$, was plotted in this work because of a time limitation. Equations (8) and (9) were solved with the aid of the IBM 650 and a program written in the ForTransit System. ForTransit was chosen at this point for greater machine speed.

The program utilized a finite summation in which small squares were taken, the configuration factors were calculated for each square, and these were then summed. The program had a command which allowed the computer to select the proper expression for the particular square under consideration. The increments chosen for the finite summation were:

$$\Delta x_1 = 0.1, \quad \Delta x_2 = 0.1, \quad \Delta y = 0.1, \text{ and } \Delta z = 0.1.$$

The results of this calculation may be found in Appendix III.

CHAPTER IV

DISCUSSION OF RESULTS

The results of this work are limited to two very special cases. This is a result of the large amounts of machine time required to calculate each point.

The first case to be considered, the point source and a parallel disk, yielded results, much as were expected. The Lambertonian surface gave a larger value of F_{12}, than did the non-Lambertonian surface, for all values of b/a, where b is the distance between the point and the disk of radius a. The error in the assumption of the Lambertonian distribution given by

$$\text{error} = \frac{\text{Lambertonian} - \text{non-Lambertonian}}{\text{Lambertonian}}$$

increased from zero at $b/a = 0$ to a maximum of 24 per cent at $b/a = 0.6$ and then decreased for increasing values of b/a approaching 16 per cent as a limit. It is interesting to note the shape of the error curve in that the error increases very rapidly and then decreases as it approaches a limit. This allows for a ready determination of the error for values of $b/a > 2$.

The second case to be considered, perpendicular planes with one edge in common, yielded much more surprising results. For the very special case under consideration, two parameters ($L = h/w$ and $M = \ell/w$) were used to represent the data where ℓ is the length, h is the

height, and w is the width. In this case for M = 1 the non-Lambertonian surface has a larger value of F_{12} for small values of L with the Lambertonian surface giving a larger value of F_{12} as L increases. The crossing of these two curves occurs at a value of L = 1.32. The error based on the Lambertonian surface begins at zero for L = 0 and becomes a maximum of -21 per cent at L = 0.12 and then increases as L increases, approaching 1 per cent as a limit. The error is zero at L = 1.32.

The reason for the reversal of the relative position of the curves for the Lambertonian and the non-Lambertonian surfaces in the two cases may be readily seen. Notice that in case one, most of the radiation which is received was emitted at small values of θ, whereas in case two, much of the radiation which is received was emitted at large values of θ. An explanation of the crossing of the two curves in case two may be obtained by examining equation (1) and noting that $D_1(\theta_1) = \epsilon(\theta_1)/\epsilon_1$.

If two surfaces, one a Lambertonian and the other a non-Lambertonian, with a normal emissivity, ϵ_n, are considered then it is noted for the Lambertonian that $\epsilon(\theta) = \epsilon_n = \epsilon_1$ and for the non-Lambertonian,

$$\epsilon(\theta) < \epsilon_1 \quad \text{for} \quad \theta < 45^\circ$$

$$\epsilon(\theta) > \epsilon_1 \quad \text{for} \quad \theta > 45^\circ$$

and

$$\epsilon_1 > \epsilon_n$$

It now follows for the Lambertonian surface that

$$D(\theta) = \epsilon(\theta)/\epsilon_1 = 1$$

and for the non-Lambertonian surface

$$D(\theta) = \epsilon(\theta)/\epsilon_1 < 1 \quad \text{for } \theta < 45^\circ$$

$$D(\theta) = \epsilon(\theta)/\epsilon_1 > 1 \quad \text{for } \theta > 45^\circ$$

Now, for the same geometry, all the terms in equation (1) except $D(\theta)$, are the same for a Lambertonian surface as they are for a non-Lambertonian surface. It is then evident for a non-Lambertonian surface that $dA_1\, dF_{dA_1 dA_2}$ is small if $\theta < 45^\circ$ and it is larger if $\theta > 45^\circ$, than it is for a Lambertonian surface.

Additional work on this subject was performed by McQuistan (9), in which he measured the diffuse reflectance of several surfaces and materials. The configuration factor was also considered between a surface dA_1 and a finite rectangular Area A_2 in a plane perpendicular to the plane of dA_1 and with a line in the plane of dA_1 passing through one corner of A_2 and perpendicular to A_2.

An approximate solution is obtained for the particular case where the receiving wall is ten times farther away than it is tall and the emitting surface is oxidized steel at 709° K . The relative error introduced by the assumption that the surface is a perfectly diffuse emitter was calculated to be 31 per cent.

CHAPTER V

CONCLUSIONS AND RECOMMENDATIONS

Conclusions.--The purpose of this study was to investigate the error one accepts when assuming a Lambertonian surface in calculating radiant heat transfer. The results of the method used in this study indicate an error in the present methods used for the calculation of radiant heat transfer. They show this method can be applied to modern day problems with the use of high speed computers. The application will, however, be very limited in the event a computer is not available. The accuracy of this work may be somewhat doubtful because of the grid size selected in the numerical calculations, but this is a result of the large amount of computer time required to reduce the grid size. The magnitude of the error, however, is difficult to determine without results, obtained for a smaller grid size, with which to compare this work.

Recommendations.--It is recommended that much more work be done on this problem. This extension would include not only more calculations of the type presented in this study, but also more data of the type obtained by Schmidt and Eckert (1) is needed. In future problems the present work should serve merely as a guide to the solution of the problem and should be used only for the geometries and conditions for which the calculations were made.

APPENDIX

APPENDIX I

CONFIGURATION FACTOR BETWEEN AN ELEMENTAL AREA AND A PARALLEL DISK

The configuration factor between a plane elemental area, dA, and a disk of radius a, parallel to and a distance b from dA, with the normal from dA passing through the center, may be obtained as follows.

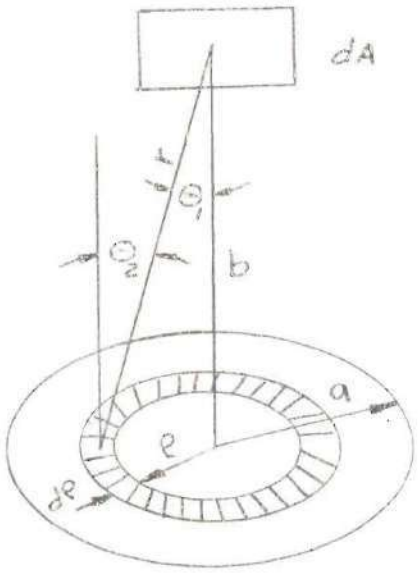

Fig. 3. Geometry for Configuration Factor Between Elemental Area and Parallel Disk

From the geometry involved the following is obtained:

$$\theta_1 = \theta_2$$

$$r = \sqrt{b^2 + \rho^2}$$

$$\cos \theta_1 = \frac{b}{r}$$

$$\sin \theta_1 = \frac{\rho}{r}$$

and $$dA_2 = 2\pi \rho \, d\rho$$

Now integrating equation (1) over Area A_2 and substituting for $D_1(\theta_1)$, equation (10) is obtained.

$$F_{dA_1 2} = \frac{1}{\pi \epsilon_1} \int_{A_2} \frac{\epsilon(\theta_1) \cos\theta_1 \cos\theta_2 \, dA_2}{r^2} \tag{10}$$

Substituting the above relations

$$F_{dA_1 2} = \frac{1}{\epsilon_1} \int_0^a \frac{2 \epsilon(\theta_1) b^2 \rho \, d\rho}{(b^2 + \rho^2)^2} \tag{11}$$

Now equations (4) and (5) are

$$\epsilon(\theta) = 0.0583 \qquad 0 \leq \theta \leq 0.6440 \tag{4}$$

$$\epsilon(\theta) = 0.0583 \left(\frac{0.3753}{\cos^2 \theta \sin \theta} \right)^{1/3} \qquad 0.6440 \leq \theta \leq 1.5621 \tag{5}$$

Then using

$$\cos (0.6440) = 0.79968 = \frac{b}{\sqrt{b^2 + \rho^2}}$$

$$\rho = 0.75 \, b$$

Equations (4) and (5) now become

$$\epsilon(\theta) = 0.0583 \qquad 0 \leq \rho \leq 0.75\, b \tag{12}$$

$$\epsilon(\theta) = 0.04205 \left[\frac{(b^2 + \rho^2)^{3/2}}{b^2 \rho}\right]^{1/3} \qquad 0.75b \leq \rho \leq a \tag{13}$$

with equations (12) and (13) it becomes evident that two possible cases exist for the solution of equation (11).

If $0.75\, b > a$

$$F_{dA_1 2} = \frac{1}{\epsilon_1} \int_0^a \frac{(0.0583) b^2\, 2\rho\, d\rho}{(b^2 + \rho^2)^2} \tag{14}$$

with $\epsilon_1 = 0.0706$ for chromium, equation (14) immediately integrates to

$$F_{dA_1 2} = 0.8258 \frac{a^2}{a^2 + b^2} \tag{15}$$

or noting the shape factor is a function of b/a only the complete solution may be obtained by assuming $a = 1$ and calculating $F_{dA_1 2}$ for various b and plotting $F_{dA_1 2}$ vs b/a. Then equation (15) becomes

$$F_{dA_1 2} = \frac{0.8258}{1 + b^2} \qquad \text{for } b > 1.333 \tag{16}$$

If $0.75\, b < a$

$$F_{dA_1 2} = \frac{1}{\epsilon_1}\left[\int_0^{0.75b} \frac{(0.0583)\, b^2\, 2\rho\, d\rho}{(b^2+\rho^2)^2} + \int_{0.75b}^{a} \frac{(0.034)\, b^{4/3}\, 2\rho^{2/3}\, d\rho}{(b^2+\rho^2)^{3/2}}\right] \tag{17}$$

Likewise if $a = 1$

$$F_{dA_1 2} = 0.2972 + 0.9632 \int_{0.75b}^{1} \frac{(b^4\rho^2)^{1/3}\, d\rho}{(b^2+\rho^2)^{3/2}} \tag{18}$$

for $b \leq 1.333$

since the first integral in equation (17), when evaluated, is a constant 0.2972.

APPENDIX II

CONFIGURATION FACTOR BETWEEN PERPENDICULAR PLANES

The configuration factor between a plane, A_1 and another plane, A_2 perpendicular to A_1 and with one edge in common may be obtained as follows:

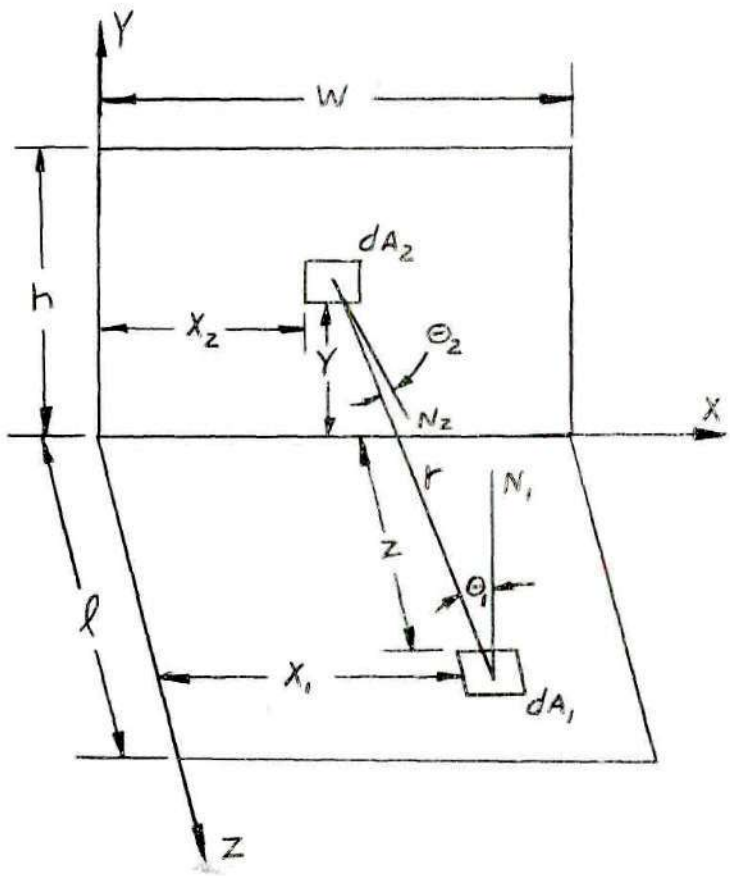

Figure 4. Geometry for Configuration Factor Between Perpendicular Planes

From the geometry involved the following relations are obtained

$$r = \sqrt{(x_1 - x_2)^2 + y^2 + z^2}$$

$$\cos \theta_1 = y/r$$

$$\cos \theta_2 = z/r$$

$$\sin \theta_1 = \frac{\sqrt{(x_1 - x_2)^2 + z^2}}{r}$$

$$\sin \theta_2 = \frac{\sqrt{(x_1 - x_2)^2 + y^2}}{r}$$

$$dA_1 = dx_1\, dz$$

and

$$dA_2 = dx_2\, dy$$

Now substituting the above relations into equation (2)

$$F_{12} = \frac{1}{\pi \epsilon_1 A_1} \int_{A_1} \int_{A_2} \frac{\epsilon(\theta_1) \cos \theta_1 \cos \theta_2\, dA_1\, dA_2}{r^2} \qquad (2)$$

equation (19) is obtained

$$F_{12} = \frac{1}{\pi \epsilon_1 \ell w} \int_{A_1} \int_{A_2} \frac{\epsilon(\theta_1)\, yz\, dx_1\, dx_2\, dy\, dz}{\left[(x_1 - x_2)^2 + y^2 + z^2\right]^2} \qquad (19)$$

Likewise equations (4) and (5) become

$$\epsilon(\theta_1) = 0.0583 \qquad 0.79968 \leq y/r \leq 1 \tag{20}$$

$$\epsilon(\theta_1) = 0.0340 \left\{ \frac{\left[(x_1 - x_2)^2 + y^2 + z^2\right]^{3/2}}{y^2 \left[(x_1 - x_2)^2 + z^2\right]^{1/2}} \right\}^{1/3} \tag{21}$$

$$\text{for } 0 < y/r < 0.79968$$

With the two different values of $\epsilon(\theta_1)$ it becomes evident that F_{12} will be the sum of two integrals. The limits of integration may be obtained as some function of the variables involved, however this is not done since neither integral can be readily evaluated. So for convenience these two integrals will be given by equations (22) and (23) where it is simply understood that these integrals will be evaluated over the two surfaces A_1 and A_2. When $\epsilon_1 = 0.0706$ they become

$$X = \frac{0.0583}{(\pi)(0.0706)\ell w} \int_{A_1} \int_{A_2} \frac{yz \, dx_1 \, dx_2 \, dy \, dz}{\left[(x_1 - x_2)^2 + y^2 + z^2\right]^2} \tag{22}$$

and

$$Y = \left\{ \frac{0.04205}{(\pi)(0.0706)\ell\, w} \int_{A_1} \int_{A_2} \frac{y^{1/3}\, z\, dx_1\, dx_2\, dy\, dz}{\left[(x_1-x_2)^2 + z^2\right]^{1/6} \left[(x_1-x_2)^2 + y^2 + z^2\right]^{3/2}} \right\} \tag{23}$$

Now $F_{12} = X + Y$.

The solution of F_{12} was obtained by a numerical integration. This was accomplished by dividing each plane into small squares, taking a mean value for x_1, x_2, y, and z, and calculating a shape factor for the small areas. The shape factor was then the sum of each of these. The selection of this method, over say Simpson's rule, was because of the simplicity of programming the problem for the IBM 650.

APPENDIX III

Tabulated Data

b/a	$F_{dA_{12}}$ N-Lam.	$F_{dA_{12}}$ Lam.	Per Cent Error Based on Lam.
0.133	0.8164	0.9826	16.91
0.533	0.5946	0.7786	23.63
1.066	0.3691	0.4678	21.10
2	0.1671	0.2000	16.45
4	0.0491	0.0588	16.50
10	0.0083	0.0099	16.16
20	0.0025	0.0021	16.00

Table 1. Disk and Elemental Area

L	F_{12} N-Lam.	F_{12} Lam.	Per Cent Error Based on Lam.
0.2	0.1043	0.0901	-15.8
0.5	0.1705	0.1594	- 6.94
1.0	0.2167	0.2134	- 1.51
2.0	0.2437	0.2463	1.05

Table 2. Perpendicular Planes $L = h/w$ $M = \ell/w$ for $M = 1$

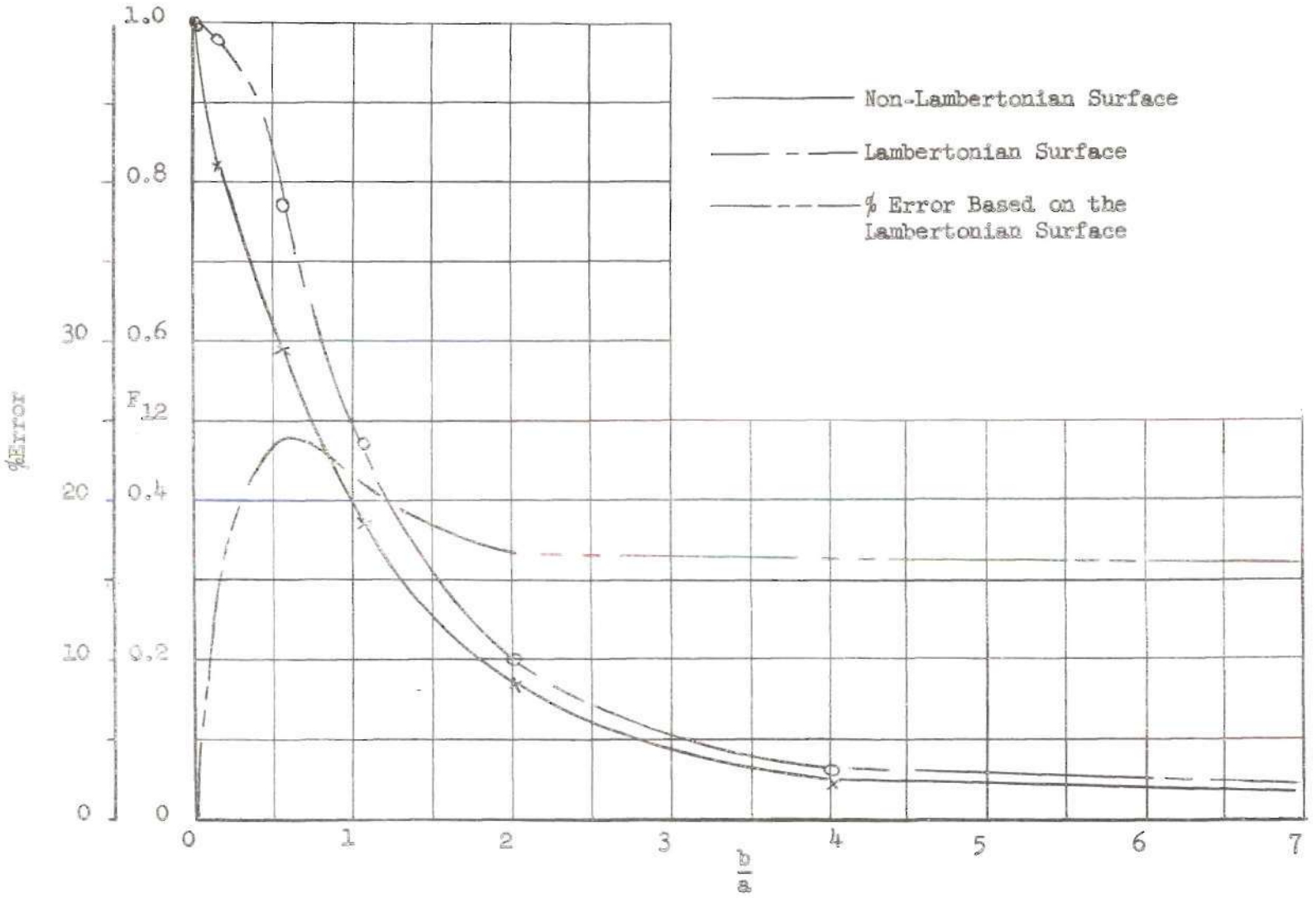

Figure 5. Shape Factor for Disk and Elemental Area

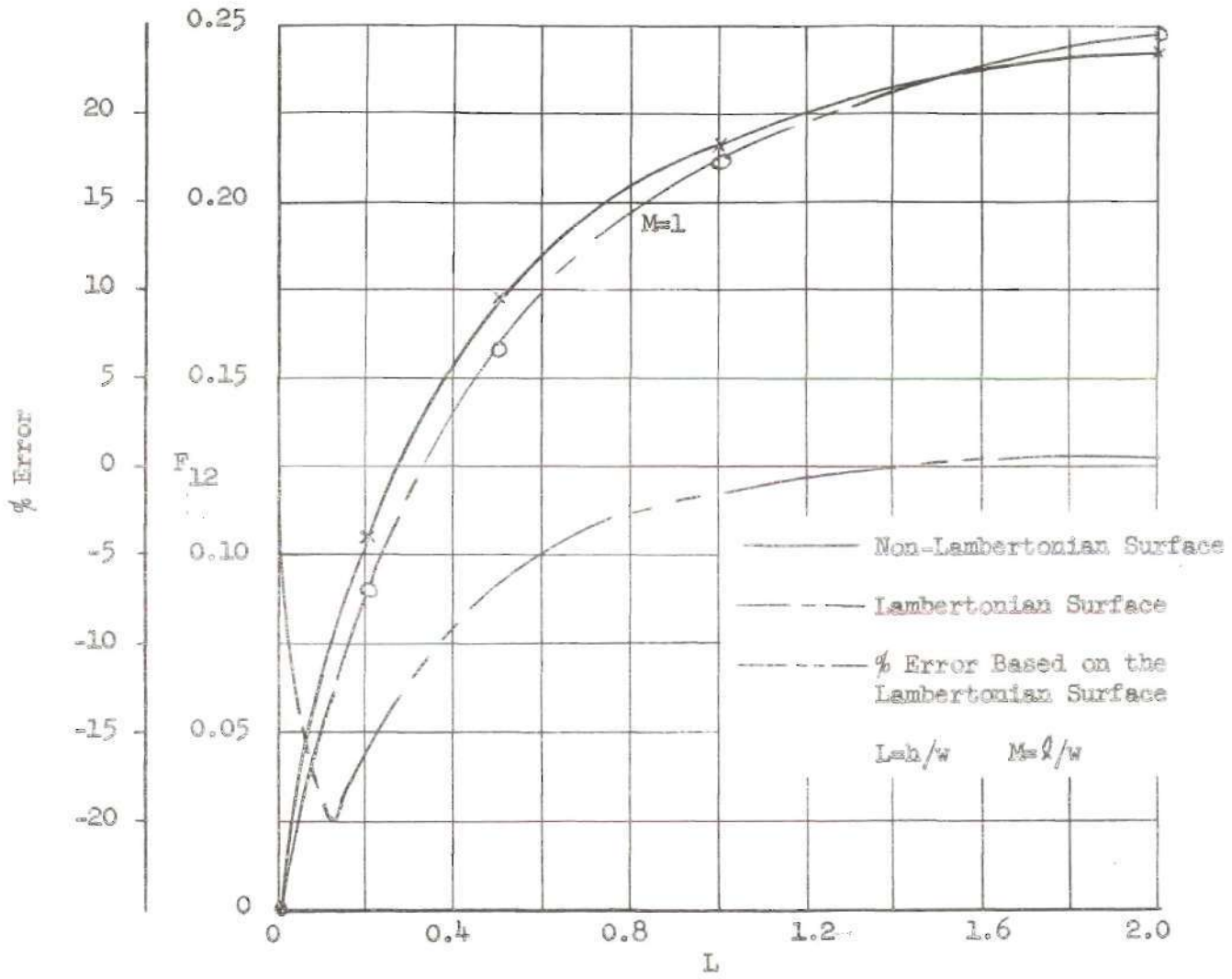

Figure 6. Shape Factor for Perpendicular Planes

BIBLIOGRAPHY

1. Schmidt, E. and Eckert, E., "Richtungsverteilung der Wärmestrahlung" Forschungsheft Gebiete Ingeuieurw. 6 (1935) p. 175.

2. Hamilton, D. C. and Morgan W. R., Radiant-Interchange Configuration Factors, National Advisory Committee for Aeronautics Technical Note 2836.

3. Eckert, E., Technische Steahlungsaustawschrechnungen und ihre Anwendeing in der Beleuchtungstechnik und beim Wärmeaustauch, VDI Verlag G. M. b. H. (Berlin), 1937.

4. Eckert, E. Introduction to the Transfer of Heat and Mass, First Edition, McGraw-Hill Book Co., Inc., 1950.

5. McAdams, W. H., Heat Transmission, Second Edition, McGraw-Hill Book Co., Inc., 1942.

6. Jakob, Max, Heat Transfer, Volume I, John Wiley & Sons, Inc., New York, 1949.

7. Jakob, Max, Heat Transfer, Volume II, John Wiley & Sons, Inc., New York, 1957.

8. Eckert, E. and Drake, R.M., Heat and Mass Transfer, Second Edition, McGraw-Hill Book Co., Inc., 1959.

9. McQuistan, R. B., "The Infrared Diffuse Reflectance Characteristics of Various Surfaces and Materials", Unpublished Ph.D. Thesis, Purdue University, 1954.